Evaluation of Absorbing Chromophores Used in Tissue Phantoms for Quantitative Photoacoustic Spectroscopy and Imaging

Jan Laufer, Edward Zhang, and Paul Beard

(Invited Paper)

***Abstract*—In this paper, the optical properties of absorbing compounds that are often used to construct tissue phantoms for quantitative photoacoustic spectroscopy and imaging are investigated. The wavelength dependence of the optical absorption of inorganic chromophores, such as copper and nickel chloride, and organic chromophores, such as cyanine-based near infrared dyes, was measured using transmittance spectroscopy and compared with that determined using photoacoustic spectroscopy. In addition, the relative change in the Grüneisen coefficient of these solutions with concentration was determined. The sound speed of aqueous gels and lipid emulsions as a function of concentration was also measured. It was found that copper and nickel chloride are suitable chromophores for the construction of photoacoustic tissue phantoms due to their photostability. By contrast, organic dyes were found unsuitable for quantitative photoacoustic measurements due to optically induced transient changes to their absorption spectrum and permanent oxidative photobleaching.**

***Index Terms*—Photoacoustic spectroscopy.**

I. Introduction

MULTIWAVELENGTH photoacoustic imaging can provide measurements of absolute concentrations of chromophore, such as oxy- and deoxyhemoglobin, in biological tissue from which related physiological parameters, such as blood oxygenation, can be obtained. In addition, the concentration of contrast agents can be obtained. The principle of this technique relies on exploiting the spectroscopic specificity of the constituent chromophores. By using their known absorption spectra as prior information in model-based inversion schemes, multiwavelength photoacoustic imaging has the potential to recover 3-D maps of the distribution of the concentration of each individual chromophore. The inversion usually incorporates a forward model, which predicts multiwavelength images or signals as a function of the spatial distribution of chromophore concentrations. The model is inverted by varying the concentrations until the difference between the measured data and that predicted by the model is minimized.

Manuscript received July 28, 2009; revised August 24, 2009; accepted August 26, 2009. Date of publication February 8, 2010; date of current version June 4, 2010. This work was supported by King's College London and UCL Comprehensive Cancer Imaging Centre CR-UK & EPSRC, in association with the MRC and DoH, U.K.

The authors are with the Department of Medical Physics and Bioengineering, University College London, London WC1E 6BT, U.K. (e-mail: jlaufer@medphys.ucl.ac.uk).

Color versions of one or more of the figures in this paper are available online at http://ieeexplore.ieee.org.

Digital Object Identifier 10.1109/JSTQE.2009.2032513

This approach has been used to, for example, determine absolute oxy- and deoxyhemoglobin concentrations, and hence blood oxygenation, from single point measurements made in tissue phantoms [1] and to recover 2-D maps of chromophore distribution from model data [2].

In order to test such methodologies, tissue phantoms with stable optical and acoustic properties are required. The spectra of the specific absorption coefficients of the different chromophores are particularly important. In this paper, the absorption spectra of chromophores commonly used in the construction of tissue phantoms were measured and their stability under pulsed optical illumination was assessed. In addition, the Grüneisen coefficients of some the chromophore solutions were determined, and the speed of sound in gels and lipid emulsions was measured. The latter are often used to construct tissue phantoms by submerging tubes filled with absorbing liquids.

II. Materials

Three cyanine-based organic dyes and three inorganic absorbers were evaluated in this paper. The dyes were S109564 (Avecia), which provides broadband absorption across the visible and nearinfrared spectrum, and two dyes (ADS740WS, ADS830WS, American Dye Source) with relatively narrow absorption bands in the nearinfrared region. The inorganic absorbers were copper chloride, nickel chloride, and Prussian blue (Sigma–Aldrich). S109564 was dissolved in distilled water at concentrations of 0.5 and 2.0 $g{\cdot}L^{-1}$, while ADS780WS and ADS830WS were dissolved in methanol at concentrations of 0.038 and 0.034 $g{\cdot}L^{-1}$, respectively. The use of methanol was necessary since it was found that the absorption spectra of ADS780WS and ADS830WS solutions are affected by the type of solvent. For example, when dissolved in water, the spectra of these dyes can be affected by dimerization and self-aggregation of cyanine dye molecules [3]. Using methanol ensured that these effects were minimized and that the absorption spectra of the dyes agreed with those provided by the manufacturer. Solutions of copper chloride, nickel chloride, and Prussian blue were made using distilled water with concentrations up to 107, 158, and 0.17 $g{\cdot}L^{-1}$, respectively. Although Prussian blue is classified as insoluble, the dry material nevertheless consists of crystals of a size small enough to readily form colloidal aqueous suspensions with a spatial homogeneity comparable to dye solutions.

The speed of sound was measured in two materials, a lipid emulsion (Intralipid, Fresenius-Kabi) and aqueous gels.

Intralipid was diluted with water to obtain lipid concentrations ranging from 5 to 20vol.%, while aqueous gels were made using bovine gelatine (Sigma–Aldrich) at concentrations ranging from 30 to 100 mg·mL^{-1}.

III. Methods

This section describes the experimental techniques with which the different materials were evaluated. This involved measurements of the absorption spectra of the different dyes using transmittance and photoacoustic spectroscopy (Section III-A), and an assessment of the effect of the concentration of the copper and nickel chloride on the Grüneisen coefficient (Section III-B). In addition, the speed of sound was measured in diluted intralipid suspensions and aqueous gels (Section III-C).

A. Measurement of Absorption Spectra

Transmittance spectroscopy, in which the attenuation spectrum of a nonscattering sample is obtained from measurements of the incident and transmitted light intensity, is the gold standard technique against which the results obtained using photoacoustic spectroscopy were compared. Photoacoustic spectroscopy was used to measure two quantities: 1) the absolute absorption coefficient spectrum, which was determined from the time-course of the photoacoustic signal; and 2) the relative photoacoustic signal amplitude spectrum, which is considered proportional to the absorption spectrum.

1) Transmittance Spectroscopy: The wavelength dependent natural attenuation, $A(\lambda)$, of the chromophore solutions was measured in quartz cuvettes of 10 mm pathlength using a dual beam spectrometer (Lambda 25, Perkin–Elmer) for wavelengths ranging from 500 to 1100 nm. For measurements in nonscattering media, $A(\lambda)$ is given by

$$A(\lambda) = \ln\left(\frac{I_0}{I}\right) = \mu_a(\lambda) l = \alpha(\lambda) c l \tag{1}$$

where I_0 is the light intensity incident on the cuvette, I is the transmitted intensity, $\alpha(\lambda)$ is the specific absorption coefficient, c is the chromophore concentration, and l is the pathlength. The specific absorption coefficient (units: L·g^{-1}·mm^{-1}), which relates the concentration of a chromophore to c, is then obtained from the measured $\mu_a(\lambda)$ using the known c of the measured sample solution and l.

2) Photoacoustic Spectroscopy: Photoacoustic signals were generated in the absorbing solutions and acquired as a function of excitation wavelength using the experimental setup shown in Fig. 1. A tuneable optical parametric oscillator (OPO) laser system (GWU, Spectra-Physics) provided 7 ns excitation pulses at wavelengths between 740 and 1040 nm. The output of the OPO was coupled into a 1.5 mm inner diameter fused silica fiber to homogenize the beam. The output of the distal end of the fiber was directed onto the surface of the absorbing solution. The fluences incident on the targets ranged from 20 to 160 mJ·cm^{-2}. The generated photoacoustic signals were detected using a Fabry–Perot ultrasound transducer with a detection bandwidth of 20 MHz. The transduction mechanism of the sensor is based on the interferometric detection of acoustically induced changes in the optical thickness of a 40-μm parylene film sandwiched between two dielectric mirrors [4]. The waveform acquisition and the wavelength tuning of the OPO were controlled using LabView. The excitation wavelength was measured using a spectrometer (EPP2000, StellarNet, Inc.). A small portion of the incident beam was directed via a beam splitter onto an integrating sphere where the intensity was measured with a reference photodiode. The photodiode output was captured simultaneously with a photoacoustic signal and subsequently used to normalize the detected waveforms with respect to the incident pulse energy.

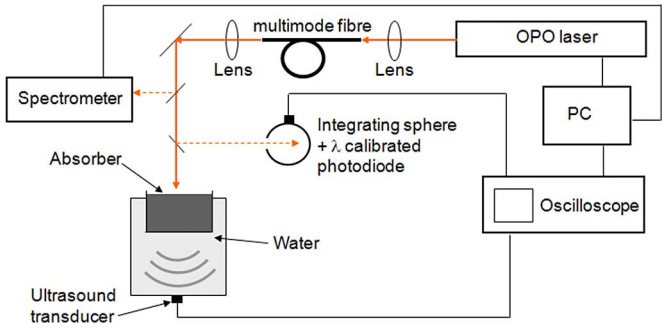

Fig. 1. Experimental setup for the measurement of photoacoustic signals generated in nonscattering liquid absorbers as a function of wavelength.

Two parameters were extracted from the detected photoacoustic signals: 1) the peak-to-peak signal amplitude; and 2) the absorption coefficient, as illustrated in Fig. 3. The absorption coefficient was obtained by fitting an analytical expression (2) of the photoacoustic signal amplitude, S, to the initial compressive part of the photoacoustic signal [5]. For nonscattering absorbers illuminated by a collimated beam at normal incidence, the photoacoustic signal amplitude can be described as

$$S(t) = K e^{-\mu_a c_s (t - t_0)} \tag{2}$$

where c_s is the speed of sound, t is time, t_0 is the time-of-arrival of the part of the wave that originated at the surface of the absorber and K is a constant, which includes for example the acoustic sensitivity of the detection system, the fluence at the surface and the Grüneisen coefficient Γ. Fitting this equation to the initial compressive part of the photoacoustic signal allows μ_a to be obtained. To obtain an estimate of the uncertainty in the determined μ_a based on the error in the measurement, its variance was calculated using methods described in [5].

By plotting the wavelength dependence of the two extracted parameters, the peak-to-peak signal amplitude and the determined μ_a, two different sets of data are obtained: the relative amplitude spectrum (obtained from the peak-to-peak amplitude measurements), and the absolute absorption coefficient spectrum (obtained from the determined values of μ_a). While the relative amplitude spectrum, which is related to the absorbed energy at the surface of the sample, does not represent an absolute measure of optical absorption, it is nevertheless proportional to $\mu_a(\lambda)$.

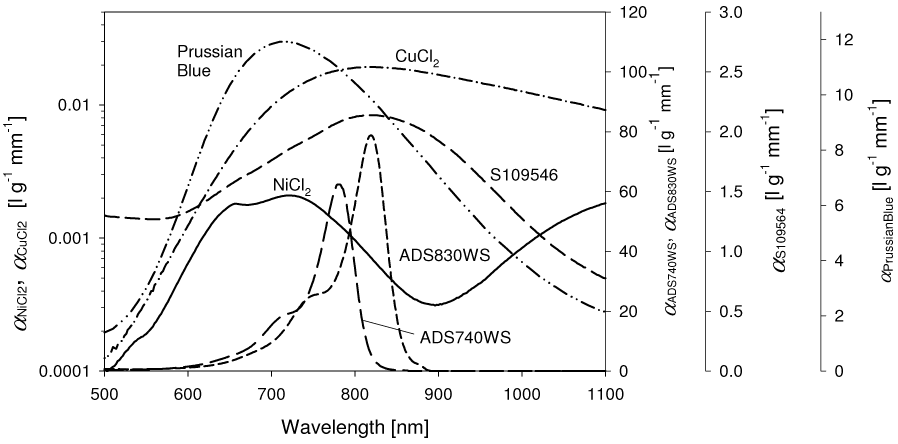

Fig. 2. Specific absorption coefficient spectra of the cyanide-based dyes S109564, ADS830WS, ADS740WS, and the inorganic absorbers $CuCl_2$, $NiCl_2$, and Prussian blue obtained using transmittance spectroscopy.

B. Measurement of the Concentration Dependence of the Grüneisen Coefficient of Copper and Nickel Chloride Solutions

Since copper and nickel chloride are weakly absorbing chromophores, it was necessary to make relatively concentrated solutions (>20 g·L^{-1}) in order to obtain $\mu_a > 0.3$ mm^{-1}. At such high concentrations, the thermomechanical properties of the solution can no longer be assumed similar to those of water. This can lead to inhomogeneities in the spatial distribution of the speed of sound or the Grüneisen coefficient within a phantom, which need to be accounted for. While there is a significant amount of literature on the change of the speed of sound with concentration of colored salts [6]–[8], information on the Grüneisen coefficient of these solutions is not available. In this study, Γ was determined by measuring the change in the photoacoustic signal amplitude as a function of concentration of copper chloride c_{Cu}, and nickel chloride c_{Ni}. The measurements were made for c_{Cu} ranging from 0 to 107 g·L^{-1} and c_{Ni} ranging from 0 to 158 g·L^{-1}. An excitation wavelength of 1450 nm, which coincides with a peak in the optical absorption of water, was used to generate the photoacoustic signals. At this wavelength, copper and nickel chloride produce a negligible μ_a (<0.05 mm^{-1}) compared to that of water (2.9 mm^{-1}) over the range of concentrations studied. Any change in the photoacoustic signal amplitude with c_{Cu} or c_{Ni} is, therefore, due to a change in Γ. By plotting the signal amplitude as a function of concentration and using linear regressions through each data set, coefficients for the change in Γ relative to that of distilled water were obtained for each chromophore. Γ can then be expressed using

$$\Gamma(c_{\mathrm{Cu}}, c_{\mathrm{Ni}}) = \Gamma_{\mathrm{H_2O}}(1 + \beta_{\mathrm{Cu}} c_{\mathrm{Cu}} + \beta_{\mathrm{Ni}} c_{\mathrm{Ni}}) \qquad (3)$$

where β_{Cu} and β_{Ni} are the coefficients of the change in Γ with c_{Cu} and c_{Ni} relative to that of water $\Gamma_{\mathrm{H_2O}}$.

C. Measurement of the Speed of Sound in Gelatine and Intralipid

Measurements of the speed of sound were made on two materials: water-based gels and intralipid. The dependence of c_s on gelatine and lipid concentration was obtained from the difference in the transit times of photoacoustic waves traveling a fixed distance through the materials compared to that in distilled water.

Photoacoustic waves were generated by illuminating a layer of black paint deposited on a block of transparent polycarbonate with nanosecond laser pulses. The paint layer, which was in contact with the sample, was positioned at a fixed distance of approximately 11 mm from the detector. The incident light had a Gaussian distribution with a e^{-2} beam diameter of 4 cm. The absorption of the optical energy generated an acoustic plane wave, which propagated through the sample and was detected using the Fabry–Perot ultrasound transducer described in Section III-A2. The time-of-arrival of the photoacoustic wave was measured in distilled water and in samples of different gelatine or lipid concentration. Since the source-detector distance was constant, it was sufficient to use the relative change in the time-of-arrival in the gel and intralipid samples to that measured in distilled water [9] to quantify the change in c_s as a function of gelatine and lipid concentration. Single optical pulses were used to generate the photoacoustic waves to avoid heating the samples. All measurements were performed at a constant temperature in the materials of 21 °C.

IV. Results

The specific absorption coefficients obtained from the transmittance measurements are presented in Section IV-A. Section IV-B presents the absolute and relative absorption spectra of solutions of organic dyes and inorganic absorbers measured using photoacoustic spectroscopy. The dependence of the Grüneisen coefficient on chromophore concentration is presented in Section IV-C, the dependence of the sound speed on gelatine and intralipid concentration is presented in Section IV-D.

A. Specific Absorption Coefficient Spectra Obtained from Transmittance Spectroscopy

The specific absorption coefficient spectra of all the chromophores obtained using transmittance spectroscopy are shown in Fig. 2. Note that the cyanine-based organic dyes typically

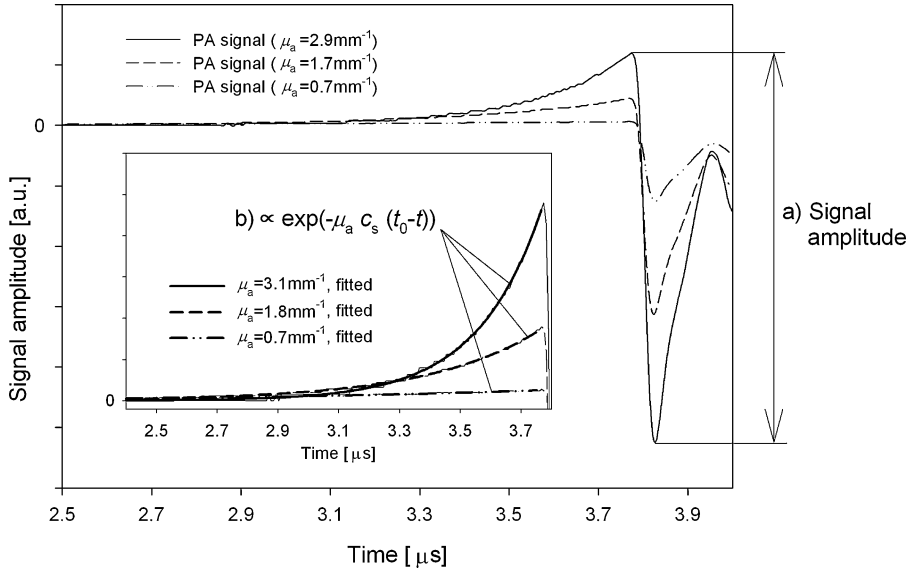

Fig. 3. Photoacoustic signals generated at 820 nm in three copper chloride solutions of different μ_a, inset shows the initial compressive part of the detected waveforms. Two parameters were obtained from the signal: (a) signal amplitude and (b) absorption coefficient, which was determined by fitting an exponential equation to the initial compressive part of the photoacoustic signal (thick line).

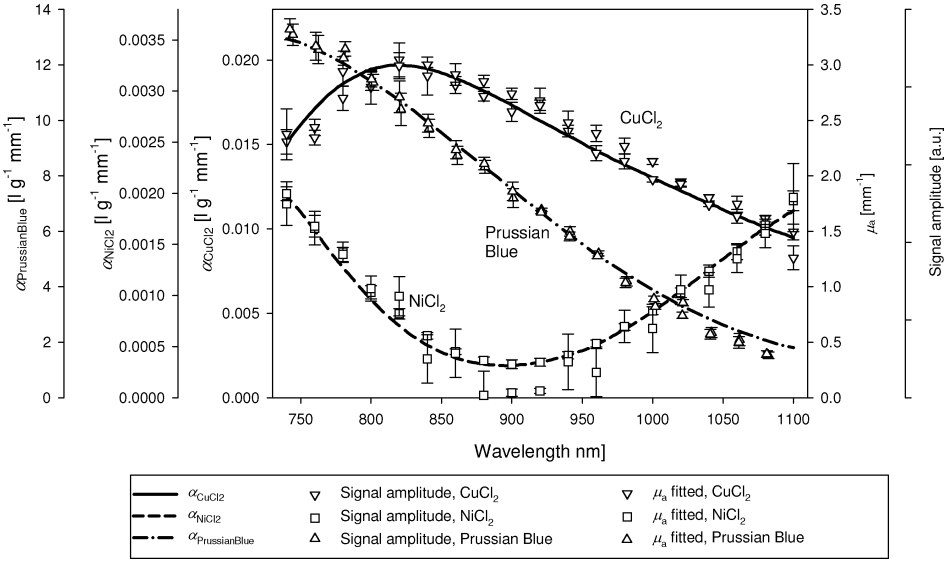

Fig. 4. Photoacoustic signal amplitude and μ_a spectra measured in copper chloride, nickel chloride, and Prussian blue solutions compared with their specific absorption spectra, which are indicated by the thick lines. The error bars of the signal amplitude spectra represent the standard deviation of three measurements, while those of the μ_a spectra represent the uncertainty in the determined values.

provide greater maximum specific absorption coefficients than inorganic absorbers. For example, the maximum $\alpha(\lambda)$ of ADS830WS is more than four orders of magnitude greater than that of nickel chloride.

B. Photoacoustic Absorption Spectra

The wavelength dependence of the specific absorption coefficients of all chromophores presented in Section IV-A is now compared to photoacoustically measured spectra of the signal amplitude and absolute μ_a. The results obtained in solutions of inorganic absorbers are presented first followed by the results measured in organic dyes.

1) Inorganic Absorbers: Fig. 3 shows photoacoustic signals detected in solutions of copper chloride of different concentrations. Two parameters were extracted from the signals: 1) the peak-to-peak signal amplitude; and 2) the absorption coefficient. The inset shows the initial compressive part of the waveforms to which (2) was fitted to determine μ_a with good agreement between the detected signal and the fitted exponential functions for all concentrations. More importantly, the determined μ_a agree well with the true values with an accuracy of better than 7%.

By repeating these measurements between 740 and 1040 nm and by plotting the signal amplitude and the determined μ_a as a function of wavelength, absolute and relative photoacoustic absorption spectra were obtained. Fig. 4 shows the photoacoustic

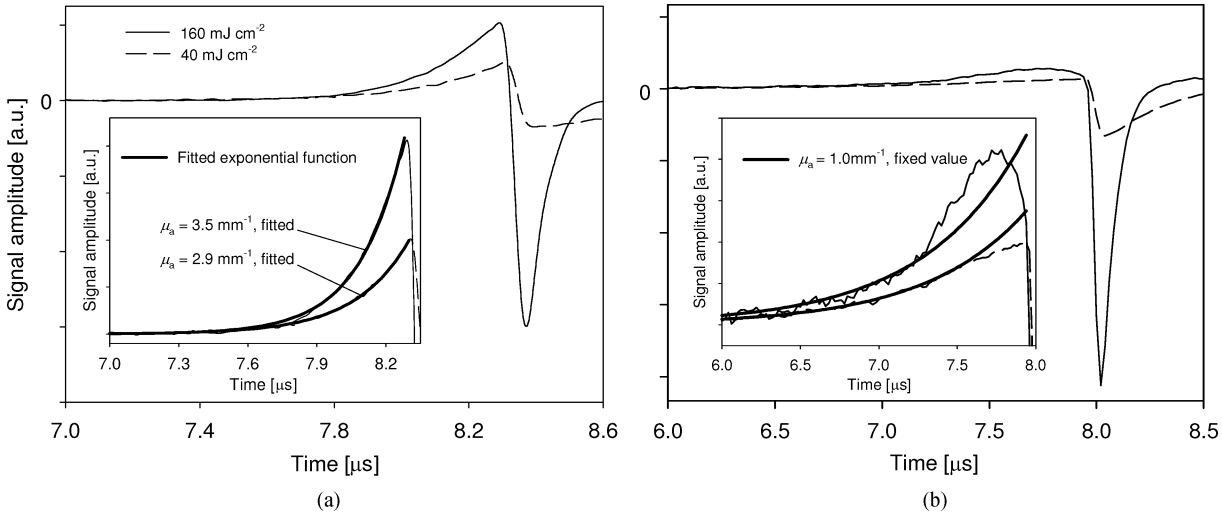

Fig. 5. Photoacoustic signal detected in solutions of S109564 with (a) $c = 2.0$ g·L^{-1} ($\mu_a = 3.1$ mm^{-1}), (b) $c = 0.5$ g·L^{-1} ($\mu_a = 1.0$ mm^{-1}) at an excitation wavelength of 820 nm and fluence levels of 40 and 160 mJ·cm^{-2}, respectively. The insets show the initial compressive part of the signals together with the exponential function (thick solid line), which was either fitted to the data (a) or evaluated for a fixed μ_a of 1 mm^{-1} (b).

spectra measured in copper chloride, nickel chloride, and Prussian blue solutions, which agree well with their specific absorption spectra measured using transmittance spectroscopy (Section III-A1). An exception is the spectrum of the nickel chloride solutions, which deviates from $\alpha_{\mathrm{NiCl}_2}(\lambda)$ between 840 and 960 nm. However, these errors are largely due to the low μ_a of the solution, and hence low signal-to-noise ratio, in this wavelength region. It is also worth noting that these measurements were independent of the incident fluence. This is in contrast to organic dyes, which are discussed in the next section.

2) Organic Dyes: Fig. 5(a) shows photoacoustic signals generated in a solution of S109564 with $\mu_a = 3.1$ mm^{-1} with fluences of 40 and 160 mJ·cm^{-2} at a wavelength of 820 nm. The inset shows the initial compressive part of the waveforms to which (2) was fitted. The values of μ_a, thus determined, fell within 13% of the known value. For the signals shown in Fig. 5(a), the agreement with the exponential function is generally good, although at a fluence of 160 mJ·cm^{-2}, a slight deviation of the photoacoustic signal from the expected exponential waveform is noticeable. This is markedly different from the signals detected in a solution with $\mu_a = 1.0$ mm^{-1} as shown in Fig. 5(b). The inset shows the compressive part of the waveform together with the waveform predicted by (2) for a fixed μ_a of 1.0 mm^{-1}. The time-course of the initial compressive part of the signals deviates significantly from the expected exponential shape. For the signal generated at 40 mJ cm^{-2} [Fig. 5(b)], the deviation from the expected exponential time-course is greatest between 7.5 and 8 μs. This corresponds to the region immediately below the illuminated surface where the fluence in the dye solution is relatively high. The deviation between the detected signal and the predicted time-course is even greater when the solution was illuminated with a fluence of 160 mJ·cm^{-2}.

Explanations for these observations may be found in the relaxation processes of the dye molecules from a photoexcited state. As well as the immediate relaxation to the ground state, some cyanine dyes have been reported to relax via the temporary formation of a photoisomer, i.e., a compound with the same molecular formula but a different structure and thus a different absorption spectrum [10], [11]. Since these isomers are temporary structures with lifetimes of up to several microseconds, transient changes in the absorption spectrum of the dye are produced. As the isomer lifetime can be longer than the duration of the optical excitation pulse, temporary changes in μ_a may be the result. Similar effects can also be produced as a result of the aggregation of dye molecules [3]. It has been suggested that the close proximity of dye molecules provides alternative pathways for the deactivation of the excited dye aggregates, causing transient absorption spectra with lifetimes of up to several nanoseconds [12], [13]. The transient change in μ_a produced by these relaxation processes has also been shown to increase with incident fluence [10], [12], which would provide a possible explanation for the results shown in Fig. 5(b).

In addition, from the differences in the photoacoustic signals shown in Fig. 5(a) and (b) it would appear that changes in μ_a are dependent not only on fluence but also on dye concentration. This may be related to a low ratio of dye molecules per unit volume to the number of photons. A large number of photons may lead to a saturation of the dye solution with isomers, leading to stronger transient changes in μ_a compared to that observed at low fluences.

Fig. 6 shows the μ_a spectra determined from measurements made at 40 mJ·cm^{-2} in a solution of S109564 with a concentration of 2 g·L^{-1} together the known absorption spectrum. Signal amplitude spectra are shown for fluences of 40 and 160 mJ·cm^{-2}. The fitted μ_a spectrum agrees well with the known absorption spectrum. However, the spectra of the signal amplitude show considerable deviation from the known μ_a, which is particularly pronounced at 160 mJ·cm^{-2}. This is likely due to transient changes in absorption, since the amplitude spectrum is obtained from the section of the photoacoustic signal that corresponds to the surface of the dye solution where the fluence is greatest.

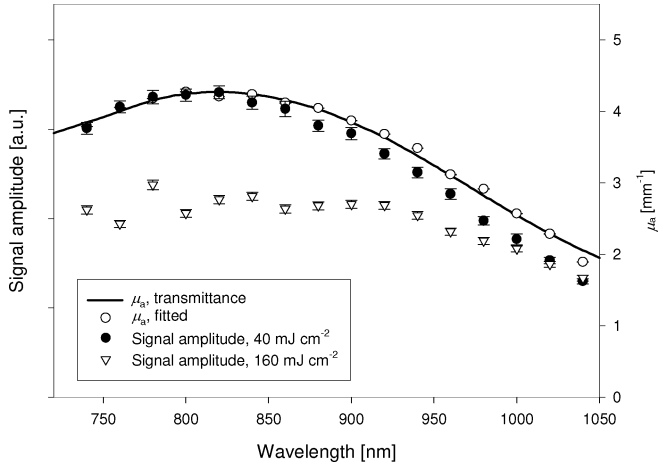

Fig. 6. Amplitude of photoacoustic signals, the fitted and the known μ_a of a solution of S109564 plotted as a function of wavelength. Spectra of the signal amplitude detected at two different fluences illustrate the effects of transient changes in μ_a at high pulse energies. The error bars of the signal amplitude spectra represent the standard deviation of ten measurements, while those of the μ_a spectra represent the uncertainty in the determined values.

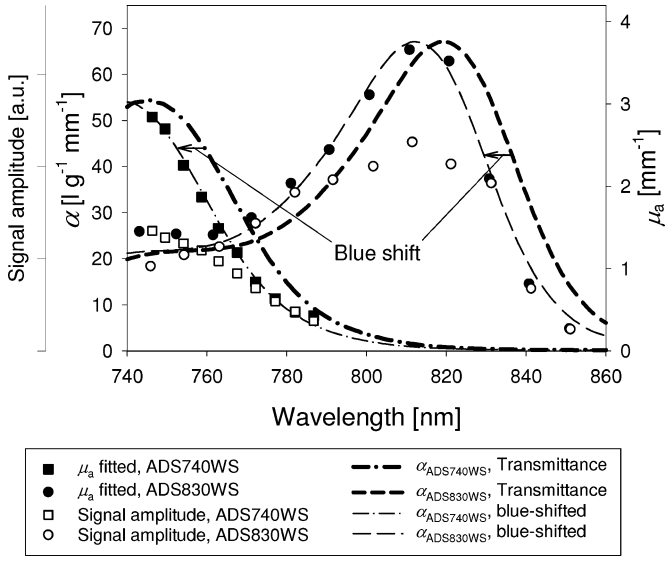

Fig. 7. Amplitude of photoacoustic signals, the fitted μ_a, and the specific absorption coefficient of solutions of ADS740WS and ADS830WS plotted as a function of wavelength. Blue shifted spectra of the specific absorption coefficient, which agree well with the spectra of the fitted μ_a, are shown to illustrate the effects of photosaturation on the absorption spectra of the dyes. Spectra of the signal amplitude illustrate the effects of optically induced transient changes in μ_a.

Similar observations were made in solutions of ADS740WS and ADS830WS. Fig. 7 shows measured photoacoustic spectra of the signal amplitude and μ_a together with the spectra of the specific absorption coefficient of these solutions.

These data show first that the measured spectra are blue-shifted by 7 nm compared with the known specific absorption spectra, which are shown by the thick lines. Such phenomena have been observed in other types of organic dyes, such as rhodamine, and have been linked to photosaturation and the interaction of the solvent with the dye [14]. Second, the signal amplitude spectra of both dyes deviate strongly from transmittance spectra. This is particularly pronounced at wavelengths that coincide with the absorption peak of each dye. This may again be due to optically induced transient changes in μ_a similar to that seen in S109564.

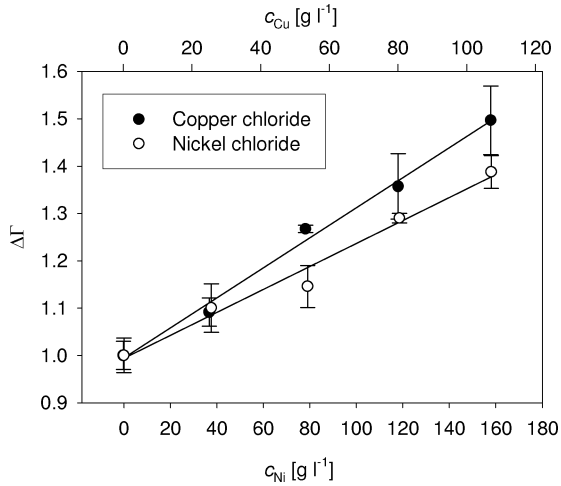

Fig. 8. Change in Γ measured in aqueous solutions of copper chloride and nickel chloride as a function of c_{Cu} and c_{Ni} relative to that of water.

It is worth mentioning that the exposure of ADS dyes to pulsed irradiation over several minutes caused permanent bleaching, which was detected as a gradual reduction in the photoacoustic signal amplitude. For cyanine dyes, this has been linked to oxidative photodegradation in which photoactivated molecules react with oxygen dissolved in the solvent [15]. In order to minimize this effect, the dyes were gently agitated during the acquisition of photoacoustic signals. Another approach is to use deoxydated solvents.

C. Concentration Dependence of the Grüneisen Coefficient of $CuCl_2$ and $NiCl_2$ Solutions

Fig. 8 shows the change in the Grüneisen coefficient with copper and nickel chloride concentration, which was found to be almost linear. Using (3), the coefficients β_{Cu} and β_{Ni} were determined as 5.8×10^{-3} L·g^{-1} and 2.25×10^{-3} L·g^{-1}, respectively. Since the absolute concentrations of organic dyes were orders of magnitude lower than those of copper and nickel chloride, the change in Γ with dye concentration is negligible. However, it should nevertheless be borne in mind that the dyes were dissolved in methanol, which has a Grüneisen coefficient[1] that is almost an order of magnitude greater than that of water [9], [16].

D. Speed of Sound in Gelatin and Intralipid

Fig. 9 shows the change in the speed of sound in aqueous gels and intralipid emulsions as a function of gelatin concentration, c_{Gel}, and lipid concentration, c_{Lipid}. The changes in c_s appear to be linear over the range of concentrations studied. However, an

[1]The absolute Grüneisen coefficient is obtained using $\Gamma = \beta c_s^2/c_p$, where β is the linear thermal expansion coefficient, c_s is the speed of sound, and c_p is the specific heat capacity.

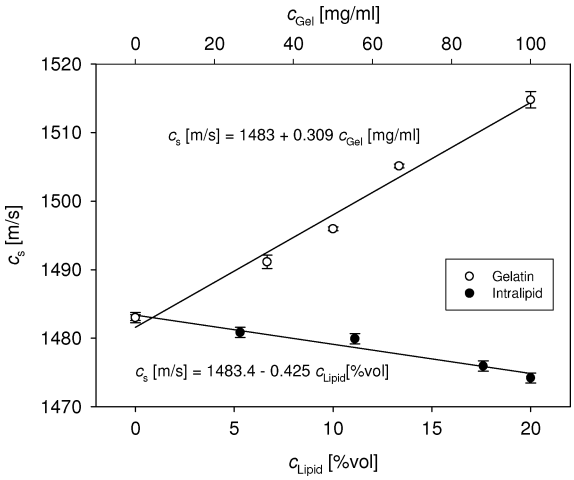

Fig. 9. Speed of sound in aqueous gels and lipid emulsions plotted as a function of gelatine and lipid concentration.

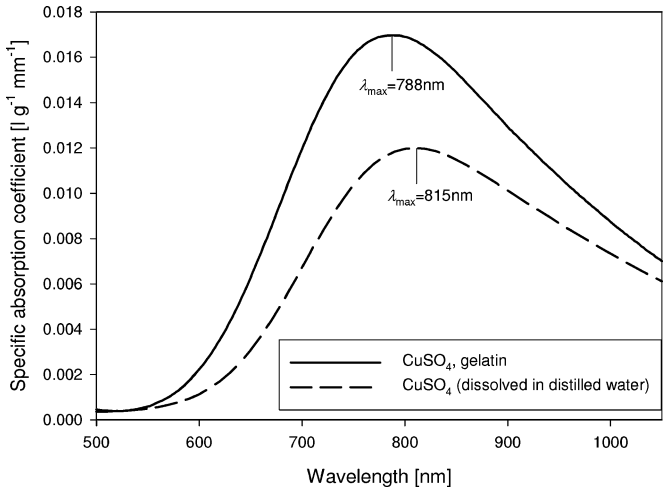

Fig. 10. Specific absorption spectrum of copper sulphate $CuSO_4$ measured in water and in an aqueous gel.

increasing gelatin concentration increases c_s, while an increase in lipid content decreases c_s. Given that typical lipid concentrations in tissue phantoms range from 1 to 5 vol%, changes in sound speed can be assumed negligible. By contrast, gels with sufficient solidity for suspending, for example, absorbing particles such as Prussian blue, require a gelatin concentration of typically between 50 and 100 mg·mL^{-1}, and this will cause a significant increase in the speed of sound compared to that of water.

E. Miscellaneous Results

As it is sometimes useful to add absorbing compounds to a scattering background medium in order to mimic, for example, the optical attenuation caused by diffusely distributed tissue chromophores, the compatibility of the absorbing chromophores with aqueous gels and intralipid was investigated.

1) Aqueous Gels Containing Copper and Nickel Salts: Aqueous gels can be useful for the suspension of scattering particles, such as titanium dioxide or microspheres. To produce a particular μ_a, it would then be advantageous to add inorganic absorbers, such as copper and nickel chloride, given that they were shown in Section IV-B1 to be very photostable. However, aqueous gels were found to react with copper or nickel ions. For example, adding copper sulphate to a gelatin and water solution caused an increase in the μ_a of the solution that was far greater than that predicted from the known concentration and specific absorption spectrum. In addition, a shift in the wavelength of maximum μ_a was also observed. This change in the optical absorption of copper ions is illustrated in Fig. 10, which shows the specific absorption spectra of copper sulphate dissolved in water and that of copper sulphate mixed with an aqueous gelatin solution.

Similar results have been reported for copper and nickel chloride [17], [18], where it was shown that the specific absorption spectra of both chromophores depend on gelatine concentration. The specific absorption spectra were also found to be affected by the relative concentrations of copper and nickel ions [17], i.e., the specific absorption coefficient of one chromophore at a particular gelatin concentration changes as a result of a variation in the concentration of the other chromophore. It has been suggested that this is due to different affinities of the metal ions to the collagen fibers. Given these complex changes, it is, therefore, not advisable to dissolve copper or nickel chloride in gelatin for making quantitative photoacoustic measurements.

2) Compatibility of Intralipid with Copper and Nickel Chloride, Organic Dyes, and Prussian Blue: The addition of copper and nickel chloride to intralipid produces turbid emulsions with optical properties that are stable for several hours. It should be noted, however, that adding only copper salts to intralipid causes lipid peroxidation. Although this was prevented to some degree using antioxidants, these emulsions were only useable for about one hour. Interestingly, the addition of nickel chloride before adding copper chloride produced an emulsion with stable optical properties lasting several days. Nickel did not appear to cause any changes in the intralipid emulsions and, in addition, seemed to prevent copper ions from causing peroxidation.

Adding the organic dyes investigated in this paper to intralipid caused gradual changes in their absorption spectrum. This may have been due to gradual oxidization and thus photobleaching but may also be related to dye molecules binding to for example the lipid droplets. The combination of organic dyes and intralipid is, therefore, useful only for photoacoustic measurement with data acquisition times of less than several minutes but does not provide a tissue phantom with long term stability in the optical properties.

Although Prussian blue was found to be a photostable chromophore, it was not used in tissue phantoms. When added to intralipid, measured data was found to deviate from results predicted using models of photoacoustic signal generation [1]. The precise reason for this was not investigated in detail but a possible explanation is that it is related to the photomagnetic properties of Prussian blue and its analogues [19], [20].

V. Discussion and Conclusion

This paper investigated a number of absorbing chromophores that can be used to construct tissue phantoms for quantitative photoacoustic imaging. The chromophores were required to be soluble and to provide reliable absorption spectra during the acquisition of photoacoustic signals. The Grüneisen coefficients of some of the absorbing solutions, and the speed of sound of gels and intralipid were also measured.

Copper and nickel chloride were found to be the most suitable chromophores for this purpose since they are water-soluble and their absorption spectra remain stable under pulsed optical irradiation. However, the relatively high copper and nickel chloride concentrations required to obtain μ_a similar to that of blood was also found to increase the Grüneisen coefficient of the solutions compared to that of water. In order to enable quantitative photoacoustic measurements, this change in Γ needed to be quantified. To this end, an empirical relationship of Γ as a function of copper and nickel chloride concentration was determined. A small number of organic, cyanine-based dyes were also evaluated and found unsuitable due to transient photodegradation and permanent oxidative photobleaching.

Intralipid provided reasonably stable scattering compound from which to make photoacoustic tissue phantoms. Its absorption spectrum, being dominated by water, is reasonably similar to that of biological tissue, and empirical relationships of the wavelength and concentration dependence of μ_s and the scattering anisotropy are available [21], [22]. In addition, the speed of sound has been found to be very close to that of water for lipid concentrations that yield μ_s similar to biological tissue.

References

[1] J. G. Laufer, D. Delpy, C. Elwell, and P. C. Beard, "Quantitative spatially resolved measurement of tissue chromophore concentrations using photoacoustic spectroscopy: Application to the measurement of blood oxygenation and haemoglobin concentration," *Phys. Med. Biol.*, vol. 52, pp. 141–168, 2007.

[2] B. T. Cox, S. R. Arridge, and P. C. Beard, "Estimating chromophore distributions from multiwavelength photoacoustic images," *J. Opt. Soc. Amer. A: Opt., Image Sci., Vis.*, vol. 26, pp. 443–455, 2009.

[3] A. Mishra, R. K. Behera, P. K. Behera, B. K. Mishra, and G. B. Behera, "Cyanines during the 1990s: A review," *Chem. Rev.*, vol. 100, pp. 1973–2011, Jun. 2000.

[4] E. Zhang, J. G. Laufer, and P. C. Beard, "Backward-mode multiwavelength photoacoustic scanner using a planar Fabry-Perot polymer film ultrasound sensor for high-resolution three-dimensional imaging of biological tissues," *Appl. Opt.*, vol. 47, pp. 561–577, 2008.

[5] J. Laufer, C. Elwell, D. Delpy, and P. Beard, "In vitro measurements of absolute blood oxygen saturation using pulsed near-infrared photoacoustic spectroscopy: Accuracy and resolution," *Phys. Med. Biol.*, vol. 50, pp. 4409–4428, 2005.

[6] S. Ernst, M. Gepert, and R. Manikowski, "Apparent molar compressibilities of aqueous solutions of $Cu(NO_3)(2)$, $CuSO_4$, and $CuCl_2$ from 288.15 K to 313.15 K," *J. Chem. Eng. Data*, vol. 44, pp. 1199–1203, Nov.–Dec. 1999.

[7] S. Ernst and R. Manikowski, "Measurements of the speed of sound and density of aqueous solutions of the first-row transition-metal halides .2. Apparent and molar compressibilities and volumes of aqueous $NiCl_2$ and $NiBr_2$ within the temperature range 291.15 K to 297.15 K," *J. Chem. Eng. Data*, vol. 42, pp. 647–650, Jul.–Aug. 1997.

[8] S. Ernst, R. Manikowski, and M. Bebek, "Measurements of the speed of sound and density of aqueous solutions of the first-row transition metal halides .1. Apparent and molar compressibilities and volumes of aqueous $CoCl_2$ and $CoBr_2$ within the temperature range 291.15 K to 297.15 K," *J. Chem. Eng. Data*, vol. 41, pp. 397–401, May–Jun. 1996.

[9] G. W. Kaye and T. H. Laby, *Tables of Physical and Chemical Constants*. White Plains, NY: Longman, 1995.

[10] R. W. Redmond, I. E. Kochevar, M. Krieg, G. Smith, and W. G. McGimpsey, "Excited state relaxation in cyanine dyes: A remarkably efficient reverse intersystem crossing from upper triplet levels," *J. Phys. Chem. A*, vol. 101, pp. 2773–2777, Apr. 10, 1997.

[11] Y. H. Meyer, M. Pittman, and P. Plaza, "Transient absorption of symmetrical carbocyanines," *J. Photochem. Photobiol. A: Chem.*, vol. 114, pp. 1–21, Mar. 31, 1998.

[12] R. F. Khairutdinov and N. Serpone, "Photophysics of cyanine dyes: Subnanosecond relaxation dynamics in monomers, dimers, and H- and J-aggregates in solution," *J. Phys. Chem. B*, vol. 101, pp. 2602–2610, Apr. 3, 1997.

[13] R. F. Khairutdinov and N. Serpone, "Laser-induced light attenuation in solutions of porphyrin aggregates," *J. Phys. Chem.*, vol. 99, pp. 11952–11958, Aug. 3, 1995.

[14] A. Marcano, N. Melikechi, and G. Verde, "Shift of the absorption spectrum of organic dyes due to saturation," *J. Chem. Phys.*, vol. 113, pp. 5830–5835, 2000.

[15] S. J. Yang, H. Tian, H. M. Xiao, X. H. Shang, X. D. Gong, S. D. Yao, and K. C. Chen, "Photodegradation of cyanine and merocyanine dyes," *Dyes Pigments*, vol. 49, pp. 93–101, May 2001.

[16] K. Tanaka, I. Fujita, and M. Uematsu, "Isobaric specific heat capacity of $\{xCH_3OH + (1 - x)H_2O\}$ with $x = (1.0000, 0.7943, 0.4949, 0.2606, 0.1936, 0.1010,$ and $0.0496)$ at $T = (280, 320,$ and $360)$ K in the pressure range from (0.1 to 15) MPa," *J. Chem. Thermodynam.*, vol. 39, pp. 961–966, 2007.

[17] W. U. Malik and M. Muzaffaruddin, "Biuret reaction of transfusion gelation .2. Influence of some bivalent metal ions on absorption spectrum of nickel-transfusion gelation complex," *J. Fur Praktische Chemie*, vol. 30, pp. 145–148, 1965.

[18] W. U. Malik and M. Muzaffaruddin, "Biuret reaction of transfusion gelatin .1. Spectrophotometric studies on interaction of copper and nickel with transfusion gelatin," *J. für Praktische Chemie*, vol. 30, p. 140, 1965.

[19] J. M. Herrera, A. Bachschmidt, F. Villain, A. Bleuzen, V. Marvaud, W. Wernsdorfer, and M. Verdaguer, "Mixed valency and magnetism in cyanometallates and Prussian blue analogues," *Philosoph. Trans. Royal Soc. A: Math. Phys. Eng. Sci.*, vol. 366, pp. 127–138, Jan. 13, 2008.

[20] S. J. Blundell, "Molecular magnets," *Contemp. Phys.*, vol. 48, pp. 275–290, Sep.–Oct. 2007.

[21] R. Michels, F. Foschum, and A. Kienle, "Optical properties of fat emulsions," *Opt. Exp.*, vol. 16, pp. 5907–5925, 2008.

[22] H. J. van Staveren, C. J. M. Moes, J. van Marle, S. A. Prahl, and M. J. C. van Gemert, "Light-scattering in intralipid 10% in the wavelength range of 400–1100 nm," *Appl. Opt.*, vol. 30, pp. 4507–4514, 1991.

Jan Laufer obtained the Diplom-Ingenieur degree in biomedical engineering from the Fachhochschule Lübeck, Lübeck, Germany, in 1995, and the Ph.D. degree in biomedical optics from University College London, London, U.K., in 2000.

Since 2002, he is a Senior Research Fellow in the photoacoustic imaging group, in the Department of Medical Physics and Bioengineering, University College London. His current research interest includes quantitative photoacoustic imaging.

Edward Zhang received the B.Eng. degree in electrical and electronic engineering from Hunan University, Changsha, China, in 1982, and the M.Sc. degree from Shanghai University of Technology, Shanghai, and the Ph.D. degree from the City University, London, U.K., both in measurement and instrumentation, in 1985 and 1994, respectively.

He was a Postdoctoral Research Fellow with the City University during 1993–2000, where he was engaged in the field of fiber optic fluorescence thermometry. From 2000 to 2002, he was with Nortel Networks, Maidenhead at the Harlow Laboratories, Harlow, where he was engaged in the optical amplifiers and optical fiber transmissions. Since 2003, he is a Senior Research Fellow in the Department of Medical Physics and Bioengineering, University College London, London. His current research interest includes photoacoustic technology for ultrasound field for biomedical imaging applications.

Paul Beard received the B.Sc. and Ph.D. degrees in physics.

He is a Professor of Biomedical Photoacoustics in the Department of Medical Physics and Bioengineering at University College London, London, U.K. His research interests include in photoacoustic imaging and spectroscopy and optical ultrasound sensing.